Single-cell DNA sequencing reveals distinct molecular types of basal cell carcinoma with unique transcriptome features

B. Bakker[1], J. Terra[2,*], L. Zhou[1,*], E. Rácz[2,*], S. Paljić, J. Garcia-Martinez, V. Oliveira, P. L. Bakker[1], D.C.J. Spierings[1], M. F. Jonkman[2], F. Foijer[1,‡]

1 European Research Institute for the Biology of Ageing, University of Groningen, University Medical Centre Groningen, A. Deusinglaan 1, Groningen, 9713 AV, The Netherlands

2 Department of Dermatology, University of Groningen, University Medical Centre Groningen, Hanzeplein 1, Groningen, 9713 GZ, The Netherlands

* These authors contributed equally to this work.

‡ To whom correspondence should be addressed: f.foijer@umcg.nl

Abstract

Background

Aneuploidy, a hallmark of cancer, is the result of chromosomal instability (CIN) during mitosis. While some aneuploid cancers display stable karyotypes, other tumours display cell-to-cell karyotype variability indicative of CIN. CIN cancers are typically associated with poor clinical outcome, as they are endowed with the potential to adjust their genomes to changing conditions including therapy. To further explore this, we assessed the degree of aneuploidy and CIN in basal cell carcinoma (BCC) and investigated whether the karyotypic makeup of tumours was associated with distinct transcriptional responses.

Patients and Methods

Samples from 11 BCC patients were processed for single-cell whole genome sequencing (scWGS) to measure aneuploidy and karyotype heterogeneity. In parallel, samples were processed for transcriptome analysis.

Results

scWGS revealed different grades of aneuploidy between BCCs, ranging from euploidy to tumours with up to 7 aneusomic chromosomes. Importantly, a subset of BCCs displayed intratumour karyotype heterogeneity, indicating that CIN can play a role in BCC. Samples were clustered into three groups based on the level of aneuploidy and intratumour karyotype heterogeneity. Karyotype-driven group classification was also reflected by the tumour transcriptomes and revealed distinct gene expression signatures related to metabolism for aneuploid BCCs and a DNA damage signature for CIN BCCs.

Conclusions

While BCCs are typically classified based on histopathological features, we find that BCCs can be stratified based on karyotypic landscape. Importantly, this classification is linked to distinct molecular features and could thus be the starting point of a molecular classification system for BCC including a readout for CIN. Importantly, the approach that we have developed is broadly applicable and could therefore also improve the diagnosis and treatment of other cancer types.

Key message

Genomic heterogeneity driven by chromosomal instability (CIN) is thought to drive therapy-resistance in cancer. We studied karyotype heterogeneity and its effect on the transcriptome in the skin cancer basal cell carcinoma (BCC). We identified transcriptional signatures distinguishing aneuploid from CIN BCCs that may be useful for stratification of tumours and prediction of treatment response.

Introduction

Cancer cells frequently display chromosomal instability (CIN), the process that drives abnormal chromosome distribution during mitosis. CIN results in cells with an abnormal DNA content, *i.e.* aneuploidy. In untransformed cells, aneuploidy leads to a stress response resulting in decreased proliferation, senescence or cell death [1]. In contrast, cancer cells take advantage of CIN to drive tumorigenesis through generation of new karyotypes, providing cancer cells with great potential to acquire additional tumorigenic traits involved in *e.g.* immune evasion and resistance to chemotherapy [2–5].

Although the terms 'aneuploidy' and 'CIN' are often used interchangeably, they are in fact different phenomena as cells can be stably aneuploid without a CIN phenotype [10]. While stably aneuploid cells generally grow slower [11, 12], CIN cells often display increased cell death, presumably as a result of the emergence of unfavourable karyotypes [10, 13, 14]. It is therefore conceivable that aneuploidy and CIN provoke different responses at the RNA level in primary tumours. Understanding the contribution of stable aneuploidy to cancer development versus that of CIN will therefore help to improve treatment strategies.

The recent advent of single-cell whole genome sequencing (scWGS) technology facilitates addressing this question, as it allows to infer CIN from intratumour karyotype heterogeneity in primary tumour samples and thus discriminate stable aneuploid cancers from those exhibiting a CIN phenotype [6–9]. While several studies have investigated aneuploidy and CIN in cancer and their effects on driver mutations [4, 15], little is known on whether aneuploidy and CIN trigger distinct transcriptional responses in cancer.

In this study, we investigated this issue using primary basal cell carcinoma (BCC) samples. BCCs are epidermal tumours for which data on genome-wide cytogenetics is scarce [16, 17]. Most BCCs can be cured by complete surgical resection. However in a subset of patients surgical excision is restricted by tumour location, or have BCCs progressed towards an advanced stage and/or metastasized [18, 19]. These patients are treated with chemo- or radiotherapy, bringing along the inherent risk of developing therapy

resistance. To better understand the contribution of CIN and aneuploidy to BCC, we subjected a cohort of BCCs to single-cell whole genome sequencing (scWGS) to infer CIN and performed RNA-sequencing to measure matching transcriptomes. This revealed transcriptional signatures that discriminate aneuploid BCCs from euploid BCCs, and stably aneuploid BCCs from aneuploid BCCs exhibiting CIN, suggesting that CIN provokes a distinct transcriptional response. As CIN tumours are believed to be more aggressive and have a tendency to become drug-resistant [5, 20], a CIN-induced transcriptome could become a powerful readout for diagnosis to stratify tumours for treatment in the future.

Materials and methods

Basal cell carcinoma sample isolation and processing

BCC samples were obtained from surplus material from Mohs surgery performed at the Department of Dermatology at the UMCG, Groningen, the Netherlands. Freshly obtained samples were split for RNA-seq and scWGS. Next, samples were homogenized, processed to single cell suspensions and frozen for further analysis as described in more detail in the supplementary methods.

Single-cell whole genome sequencing and AneuFinder analysis

Samples for scWGS were processed and analysed as described before [6, 7]. Briefly, single cell suspensions were stained for DNA content, sorted into 96-well plates by flow cytometry followed by library preparation, multiplexing and sequencing. Following sequencing, data were demultiplexed, aligned, and analysed using AneuFinder [7]. More details can be found in the supplementary methods.

RNA-sequencing library preparation and analysis

For transcriptome analysis, RNA was isolated from BCC samples followed by quality control on a Bioanalyzer (Agilent). RNA sequencing libraries were prepared with poly(a) selection

using the NEXTflex kit (Bioo Scientific). Individual libraries were barcoded and pooled followed by sequencing. Demultiplexed libraries were aligned to the human reference (GRCh38) and analysed as described in detail in the supplemental methods.

Sequencing data availability

Unaligned sequencing data have been to submitted to the European Nucleotide Archive (ENA) and are available only upon request due to EU patient privacy legislation (accession number PRJEB28285).

Results

Single-cell whole genome sequencing reveals karyotype heterogeneity in BCC

Tumour samples were collected from 11 patients diagnosed with BCC alongside with healthy control tissue where possible (median age: 74.5 years, Fig. 1A). Histopathological assessment revealed that the cohort included the most common subtypes: nodular/infiltrative, infiltrative, micronodular, or nodular (Fig. 1B). To circumvent the limitations of traditional karyotyping methods [21], we subjected samples to scWGS (24 cells per sample) to quantify aneuploidy and intratumour copy number heterogeneity (Fig. 1C) [6, 22]. 72.7 ± 15.6% (mean ± SD) of the libraries passed quality control, additional scWGS quality metrics can be found in Table S1.

With the exception of BCC5, all BCCs displayed structural and/or numerical abnormalities in multiple or most cells (Fig. 1D), indicating reasonable tumour cell purity. Non-aneuploid cells in aneuploid BCCs are likely non-cancer cells that surround the cancer nodules (also see histology in Fig. 1A). Besides whole chromosome abnormalities, a subset of BCCs also harboured structural aberrations typically involving the gain or loss of whole chromosome arms, *e.g.* involving loss of Chr. 9p (Fig. 1D). Interestingly, in addition to aneuploidy, two BCCs (BCC3 and BCC9) exhibited significant karyotype heterogeneity, a strong indication for ongoing CIN [22, 23].

To stratify the BCCs based on aneuploidy and karyotype heterogeneity for subsequent transcriptional analysis, we calculated the aneuploidy and heterogeneity scores using AneuFinder [22] for the tumour karyotypes as a whole, as well as for individual chromosomes (Fig. 1E). For these calculations, euploid libraries were excluded, circumventing an impact of non-cancer cell libraries on heterogeneity scores. Together, these analyses revealed that the BCCs could roughly be grouped into three distinct karyotypic subtypes: BCCs 1, 4, 5, 6, 7, and 8 showed little to no aneuploidy, with 0 to 2 aneusomic chromosomes (group 1; near-euploid). BCCs 2, 10 and 11 displayed a much larger number of aneusomic chromosomes, but no intratumour heterogeneity (group 2; stably aneuploid). Finally, BCC3 and BCC9 displayed both multiple aneusomic chromosomes as well as intratumour heterogeneity, and were therefore classified as CIN (group 3; CIN). Together, these data reveal that basal cell carcinoma exhibit widely varying karyotypes with a subset displaying intratumor heterogeneity.

Transcriptome analysis reveals general deregulation of SHH, cell cycle, and cilia genes in BCC

To determine the impact of aneuploidy and/or CIN on the tumour transcriptomes, we next subjected a subset of BCCs from each cluster alongside with healthy control skin samples to RNA sequencing (Fig. 1C, Fig. 2A). Interestingly, principal component analysis (PCA) revealed a clear separation between karyotypic subgroups (compare Fig. 1E to Fig. 2A) indicating that CIN and aneuploidy have a strong impact on the tumour transcriptomes. We first determined which genes were significantly deregulated in BCC in general as compared to control skin. 5,197 genes were differentially expressed (DE) between healthy skin and BCC (Wald test, FDR<0.05; Fig. 2B – left panel) and enriched for functions in skin/epidermis development, cell cycle regulation, and cilium biology (Fig. 2B – right panel). This fits well with current literature, which frequently reports keratinization (epidermal development) and deregulation of the Hedgehog signalling pathway in BCC (Table S2; Fig. 2C) [16, 18, 19, 24–26].

K-means clustering reveals distinct aneuploidy- and CIN-induced transcriptome features

A large part of aneuploidy- and CIN-imposed transcriptome changes is the direct result of gained or lost alleles [27, 28]. As direct transcriptional changes might cloak secondary aneuploidy/CIN-imposed changes (*e.g.* an aneuploidy-stress response), we applied a copy number-based correction (CNC) to the gene expression dataset, normalizing the transcriptome readout to the copy number state (Fig. S1A), as explained in the supplemental methods (exemplary data in Fig. S1B; Fig. S2-S3 show complete dataset before/after CNC).

We next assessed transcriptome changes specific to near-euploid, stably aneuploid and CIN BCCs. Hereto, we performed k-means clustering [29] of the copy-number-corrected transcriptomes for all samples and transcripts, supervised according to the BCC karyotypic groups (healthy skin, near-euploid, stably aneuploid, and CIN). The optimal number of clusters, *k*, as determined by the *within group sum of squares* for different values for *k* [29], was 10 (Fig. S1C). Expression patterns per cluster were plotted between the karyotypic groups (Fig. 3A, Table S5) and clusters were analysed for biological pathway enrichment (Fig. 3B; Tables S6-S8). Cluster 7 contained genes whose expression increased in all BCCs, while transcripts in cluster 9 showed decreased expression. Indeed, cluster 7 was enriched for pathways involved in cancer and Hedgehog signalling (Fig. 3C), confirming our first analysis comparing all BCCs to healthy epidermis (compare Fig. 2C to Fig. 3C). Conversely, genes in cluster 9 were enriched for genes involved in the sphingolipid metabolism, skin barrier function and epidermal differentiation, suggesting that increasing aneuploidy contributes to epidermal barrier malfunctioning (Fig. 3D). Genes in cluster 4 displayed decreased expression in all aneuploid BCCs (stably aneuploid and CIN), suggesting that these transcripts are downregulated as a result of aneuploidy. Here, genes for metabolic pathways such as PPAR signalling and amino acid metabolism were enriched (Fig. 3B, 3E, Tables S6-8), which is consistent with other observations that aneuploidy confers a change

in metabolic state [27, 28, 30, 31]. Finally, cluster 1 contained the transcripts increased specifically in CIN BCCs, and included genes involved in DNA repair, DNA replication, homologous recombination, chromosome segregation, and the Fanconi anaemia pathway (Fig. 3B, 3F Tables S6-8), revealing a DNA damage signature for CIN tumours. Together, these data indicate that while aneuploidy provokes deregulation of the cellular metabolism, the addition of a CIN phenotype leads to upregulation of pathways involved in DNA damage in BCC.

Aneuploidy and CIN impose distinct transcriptional features upon BCC cells

We next performed a second, more stringent analysis in which we determined which genes significantly changed expression with either increasing aneuploidy (using the aneuploidy score (Fig. 1E) as a parameter) or increasing CIN (using the heterogeneity score (Fig. 1E) as a parameter). For this we employed a generalized linear model (GLM - see supplementary materials & methods) on the copy-number-corrected dataset, which revealed that only 21 genes significantly correlated with the degree of aneuploidy (Fig. S4A, B, Table S9), revealing that aneuploidy by itself has a small impact on copy-number-corrected tumour transcriptomes. When assessing which expression changes correlate with increasing heterogeneity, we found that expression of 286 genes changed (negative binomial likelihood ratio test, FDR<0.05) thus revealing a BCC CIN-signature gene set (Fig. 4A, C, Table S10). Biological pathways enriched in this 'heterogeneity signature', included cell adhesion and Rap1 signalling, which fits with increased cellular mobility and tumour aggressiveness associated with CIN tumours (Fig. 4D, Table S11) [3].

Altogether, we conclude that BCCs can be subdivided into three distinct karyotypic classes that are associated with distinct transcriptome features, with the CIN phenotype having the strongest impact on the tumour transcriptome.

Discussion

In this study we examined aneuploidy and intratumour karyotype heterogeneity in a panel of BCCs, a feature that, to our knowledge, has not been studied before for this cancer. We found that BCCs can be grouped into three karyotypic types: near-euploid, stably aneuploid, and CIN. Of note, the aneuploidy scores were similar between stably aneuploid and CIN tumours, suggesting that differences between stably aneuploid and CIN tumours are the sole consequence of the CIN phenotype.

To investigate whether aneuploidy and CIN trigger distinct transcriptional responses, we took two approaches. First, we performed global k-means clustering to determine whether expression changes in near-euploid, stably aneuploid and CIN BCCs correlated with particular biological functions. Indeed, this revealed that alterations in the Hedgehog pathway were common across all BCCs, that aneuploid BCCs exhibit a metabolic signature, and that CIN BCCs display an increase in genes involved in DNA repair. While the alterations in metabolic profile fit well with previous publications on aneuploid (cancer) cells [27, 28, 30, 31], the CIN-associated DNA signature is to our knowledge the first *in vivo* evidence confirming observations in cultured cells showing that CIN leads to DNA damage and a mutator phenotype [32–35]. However, whether the increased activity of DNA repair pathways is indeed the result of increased DNA damage *in vivo* needs further investigation.

Our findings are not only relevant for the fundamental understanding of aneuploidy and CIN in cancer, but also bear clinical relevance. For instance, several Sonic Hedgehog inhibitors are at various stages of clinical trials [18, 19] for the treatment of inoperable BCCs (for instance locally advanced or metastatic BCC) [18]. As CIN BCCs would be particularly at risk of developing resistance against such drugs, our molecular classification for BCCs (using single cell genomics, transcriptome analysis, or possibly evidence of DNA damage) could aid in predicting therapy resistance when treating patients suffering from advanced or metastatic BCC.

Acknowledgements

We would like to thank all patients that provided material for this study for their consent. In addition, we would like to thank the technicians of the single-cell sequencing facility at ERIBA, including Jennefer Beenen, Nancy Halsema, and Karina Hoekstra-Wakker. Finally, we thank the members of the Foijer, Jonkman and Bruggeman groups, and in particular Sophia Bruggeman and Michael Schubert, for helpful suggestions and fruitful discussions.

Funding

This research was supported by Dutch Cancer Society grant 2012-RUG-5549 and an NWO TOP grant 91215003 awarded to Floris Foijer and a UMCG intramural seeding grant to Floris Foijer and Marcel Jonkman.

Author contributions

J.T. and E.R. provided patient material and performed histopathological diagnosis. B.B., L.Z., S.P. J.G.M. and V.O. processed patient material. B.B. performed single-nuclei sorts and analysed sequencing data. P.L.B. performed RNA-seq library preparation. D.C.J.S. supervised scWGS and RNA-sequencing. B.B. and F.F. wrote the manuscript. M.F.J. and F.F. conceptualized the study and provided funding.

Figure legends

Figure 1: Single-cell whole genome sequencing reveals varying degrees of karyotype heterogeneity in BCC.

A. Summary information on the BCC patient sample set, as well as representative images of H&E staining. Green blocks in the table indicate whether a sample was processed for single-cell whole genome sequencing (scWGS) and RNA-sequencing. **B.** Representative images of the BCC classification, based on H&E staining. **C.** Schematic overview of the sample processing pipeline, from homogenization to library preparation for scWGS and transcriptome analysis (RNA-seq). **D.** Genome-wide copy number heatmaps of 11 BCC samples, with individual cells in rows and genome position in columns. Chromosome boundaries are indicated in black lines, with colours corresponding to the most likely assigned copy number state per 2 Mb bin as determined by AneuFinder. Percentage of aneuploidy indicates the fraction of libraries that display aneuploidy for at least 1 chromosome arm. **E.** Genome-wide aneuploidy and heterogeneity scores for the aneuploid libraries. Samples processed further for RNA-sequencing are highlighted in bold.

Figure 2: Aneuploidy and CIN-specific transcriptome signatures in basal cell carcinoma.

A. Principal component analysis (PCA) of the RNA-seq libraries, showing the percentage of contribution of PC1 and PC2 to variance, and colour-coded by group identifier. **B.** The number of significant DE genes up- and downregulated between all BCCs and healthy skin (left panel), and GO & KEGG-pathway enrichment analysis (right panels). Where indicated, columns show GO-term or KEGG pathway description, the number of observed genes, fold enrichment (FE) over expected observations, and BH-adjusted p-value (FDR). **C.** Expression heatmap of commonly deregulated genes in basal cell carcinoma, related to SHH and WNT signalling. Normalized expression values are expressed as z-scores (by gene). Gene names highlighted in bold are significantly deregulated (FDR < 0.05).

Figures 3: Copy number-corrected expression analysis of global gene expression profiles reveals a CIN-specific DNA damage signature.

A. Global gene expression profiles as determined by group-supervised k-means clustering. The number of genes in each cluster are shown in the top left of each graph. Individual black lines represent median normalized log2 gene expression across individual groups, with red lines indicating the median expression for all genes in the cluster. **B.** KEGG pathway enrichment results for all clusters, showing fold enrichment, significance (FDR) and the number of genes identified per term. **C-F**. Gene expression heatmaps of relevant pathways deregulated in BCCs. Expression values are z-scaled per gene based on normalized log2 counts. Aneuploidy, heterogeneity, and group assignment is indicated per sample.

Figure 4: Transcriptome analysis reveals a CIN-signature in BCC

A. Gene expression heatmap of 286 genes correlating significantly with heterogeneity, revealing a CIN-signature. **B.** Ordered karyotype measures as determined by scWGS (also see Fig. 1E). **C.** Normalized log2 expression values of the top 10 CIN-signature genes. **D.** Enriched GO-terms for CIN-signature genes.

References

1. Williams BR, Amon A. Aneuploidy: cancer's fatal flaw? Cancer Res. 2009; 69(13):5289–91.
2. Sansregret L, Vanhaesebroeck B, Swanton C. Determinants and clinical implications of chromosomal instability in cancer. Nat. Rev. Clin. Oncol. 2018; 15:139–150.
3. Bakhoum SF, Landau DA. Chromosomal Instability as a Driver of Tumor Heterogeneity and Evolution. Cold Spring Harb. Perspect. Med. 2017; 7:a029611.
4. Davoli T, Xu AW, Mengwasser KE et al. Cumulative Haploinsufficiency and Triplosensitivity Drive Aneuploidy Patterns and Shape the Cancer Genome. Cell 2013;

155(4):948–962.

5. McGranahan N, Rosenthal R, Hiley CT et al. Allele-Specific HLA Loss and Immune Escape in Lung Cancer Evolution. Cell 2017; 171:1–13.
6. van den Bos H, Spierings DCJ, Taudt AS et al. Single-cell whole genome sequencing reveals no evidence for common aneuploidy in normal and Alzheimer's disease neurons. Genome Biol. 2016. doi:10.1186/s13059-016-0976-2.
7. Bakker B, Taudt A, Belderbos M et al. Single cell sequencing reveals karyotype heterogeneity in murine and human tumours. Genome Biol. 2016; 17:1–15.
8. Navin N, Kendall J, Troge J et al. Tumour evolution inferred by single-cell sequencing. Nature 2011; 472(7341):90–94.
9. Gao R, Davis A, McDonald TO et al. Punctuated copy number evolution and clonal stasis in triple-negative breast cancer. Nat. Genet. 2016; 48(10):1119–1130.
10. Schukken KM, Foijer F. CIN and Aneuploidy: Different Concepts, Different Consequences. BioEssays 2017. doi:10.1002/bies.201700147.
11. Tang Y-C, Williams BR, Siegel JJ, Amon A. Identification of aneuploidy-selective antiproliferation compounds. Cell 2011; 144(4):499–512.
12. Pavelka N, Rancati G, Zhu J et al. Aneuploidy confers quantitative proteome changes and phenotypic variation in budding yeast. Nature 2010; 468(7321):321–325.
13. Libouban MAA, de Roos JADM, Uitdehaag JC et al. Stable aneuploid tumors cells are more sensitive to TTK inhibition than chromosomally unstable cell lines. Oncotarget 2017; 8(24):38309–38325.
14. Simon J, Bakker B, Foijer F. CINcere modelling: What have mouse models for chromosome instability taught us? Results Cancer Res. 2015; 200:39–60.
15. Sack LM, Davoli T, Li MZ et al. Profound Tissue Specificity in Proliferation Control Underlies Cancer Drivers and Aneuploidy Patterns. Cell 2018; 173(2):499–514.e23.
16. Jayaraman SS, Rayhan DJ, Hazany S, Kolodney MS. Mutational Landscape of Basal Cell Carcinomas by Whole-Exome Sequencing. J. Invest. Dermatol. 2014; 134:213–220.

17. Mertens F, Heim S, Mandahl N et al. Cytogenetic Analysis of 33 Basal Cell Carcinomas. Cancer Res. 1991; 51:954–957.

18. Migden MR, Lynn A, Chang S et al. Emerging trends in the treatment of advanced basal cell carcinoma. Cancer Treat. Rev. 2018; 64:1–10.

19. Kudchadkar R, Lewis K, Gonzalez R. Advances in the Treatment of Basal Cell Carcinoma□: Hedgehog Inhibitors. Semin. Oncol. 2012; 39(2):139–144.

20. McClelland SE. Role of chromosomal instability in cancer progression. Endocr. Relat. Cancer 2017. doi:10.1530/ERC-17-0187.

21. Bakker B, van den Bos H, Lansdorp PMPM, Foijer F. How to count chromosomes in a cell: An overview of current and novel technologies. BioEssays 2015. doi:10.1002/bies.201400218.

22. Bakker B, Taudt A, Belderbos ME et al. Single-cell sequencing reveals karyotype heterogeneity in murine and human malignancies. Genome Biol. 2016; 17(1):115.

23. Foijer F, Albacker LA, Bakker B et al. Deletion of the MAD2L1 spindle assembly checkpoint gene is tolerated in mouse models of acute T-cell lymphoma and hepatocellular carcinoma. Elife 2017. doi:10.7554/eLife.20873.

24. Misago N, Satoh T, Narisawa Y. Cornification (Keratinization) in Basal Cell Carcinoma□: A Histopathological and Immunohistochemical Study of 16 Cases. J. Dermatol. 2004; 31(12):637–650.

25. Goetz SC, Ocbina PJR, Anderson K V. The Primary Cilium as a Hedgehog Signal Transduction Machine. Methods Cell Biol. 2009; 94:199–222.

26. Skoda AM, Simovic D, Karin V et al. The role of the Hedgehog signaling pathway in cancer□: A comprehensive review. Bosn. J. Basic Med. Sci. 2018; 18(1):8–20.

27. Foijer F, Xie SZ, Simon JE et al. Chromosome instability induced by Mps1 and p53 mutation generates aggressive lymphomas exhibiting aneuploidy-induced stress. Proc. Natl. Acad. Sci. U. S. A. 2014. doi:10.1073/pnas.1400892111.

28. Dürrbaum M, Kuznetsova AY, Passerini V et al. Unique features of the transcriptional response to model aneuploidy in human cells. BMC Genomics 2014; 15(1):139.

29. Lucas A. Another Multidimensional Analysis Package. 2018.

30. Williams BR, Prabhu VR, Hunter KE et al. Aneuploidy affects proliferation and spontaneous immortalization in mammalian cells. Science 2008; 322:703–709.

31. Foijer F, DiTommaso T, Donati G et al. Spindle checkpoint deficiency is tolerated by murine epidermal cells but not hair follicle stem cells. Proc. Natl. Acad. Sci. U. S. A. 2013; 110(8):2928–2933.

32. Burrell RA, McClelland SE, Endesfelder D et al. Replication stress links structural and numerical cancer chromosomal instability. Nature 2013; 494(7438):492–496.

33. Ohashi A, Ohori M, Iwai K et al. Aneuploidy generates proteotoxic stress and DNA damage concurrently with p53-mediated post-mitotic apoptosis in SAC-impaired cells. Nat. Commun. 2015; 6:1–16.

34. Janssen A, van der Burg M, Szuhai K et al. Chromosome segregation errors as a cause of DNA damage and structural chromosome aberrations. Science (80-.). 2011; 333(6051):1895–8.

35. Kolodner RD, Cleveland DW, Putnam CD. Aneuploidy drives a mutator phenotype in cancer. Science (80-.). 2011; 333(6045):942–943.

A

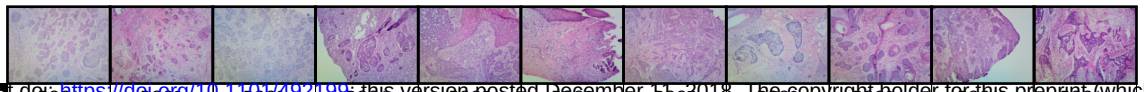

Sample ID	BCC1	BCC2	BCC3	BCC5	BCC6	BCC7	BCC8	BCC9	BCC10	BCC11
Gender	M	F	M	M	M	M	F	M	F	M
Age at time of excision (y)	77	54	78	85	58	74	41	55	75	75	89
Topography	nasal ala	temple	cheek	upper lip	chin	ear	lateral to eye	upper lip	forehead	forehead	ear
UV exposure history	low sun exposure	moderate sun exposure	high sun exposure	likes to be in the sun	high sun exposure	high sun exposure	high sun exposure (as a child)	moderate sun exposure	moderate sun	moderate sun exposure	high sun exposure
Classification	nodular (partial)	nod./infil.	micronodular	infiltrative	nod./infil.	nodular	nod./infil.	micronodular	nodular	nodular	nod./infil.
scWGS	■	■	■	■	■	■	■	■	■	■	■
RNA-seq	■	■	■		■			■	■	■	■
Matched healthy skin					■				■	■	■

B

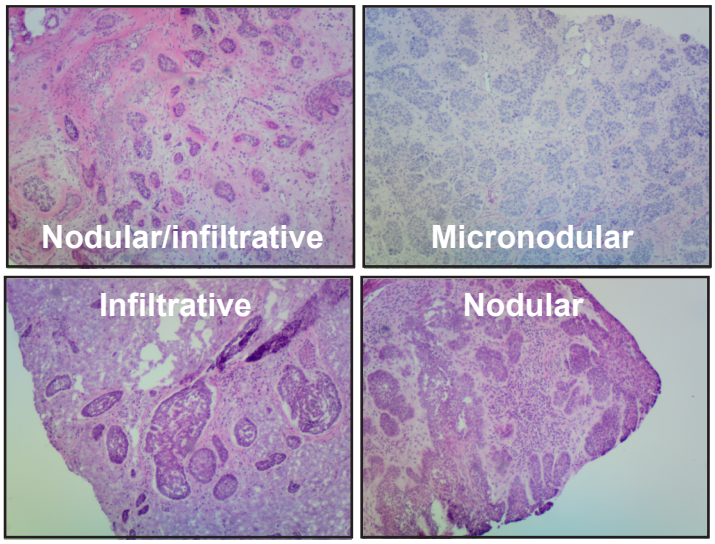

C

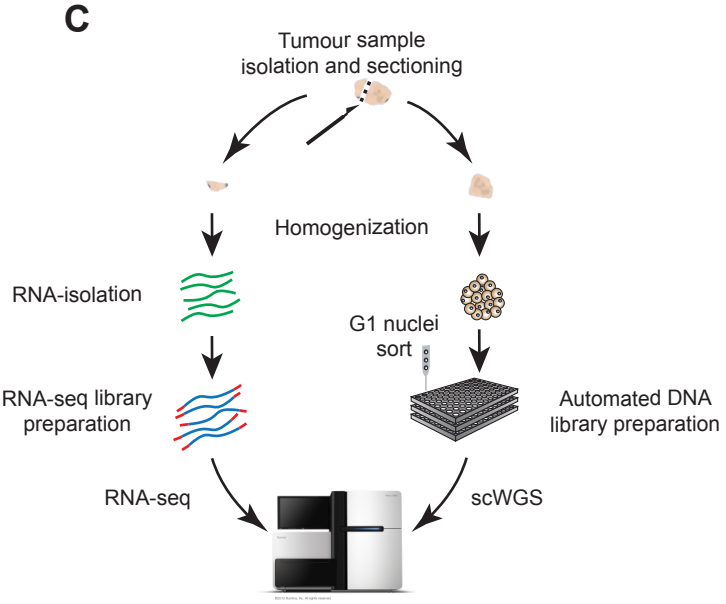

D

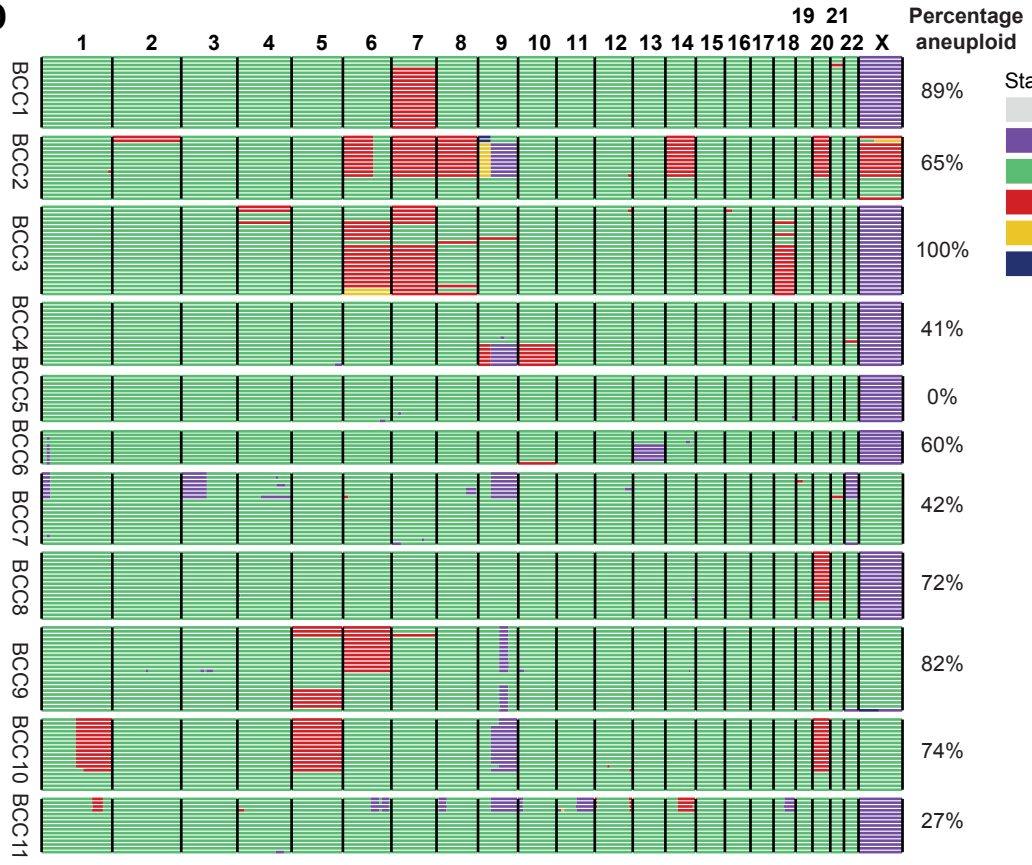

E

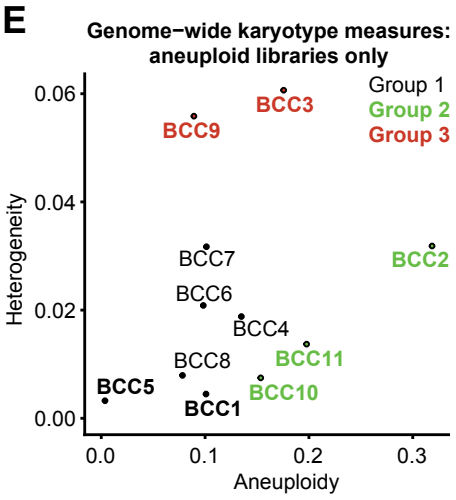

Bakker *et al*, Figure 1

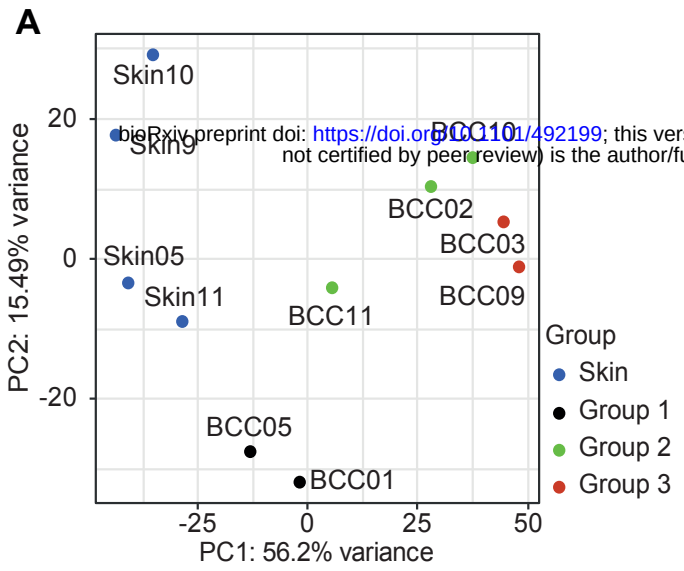

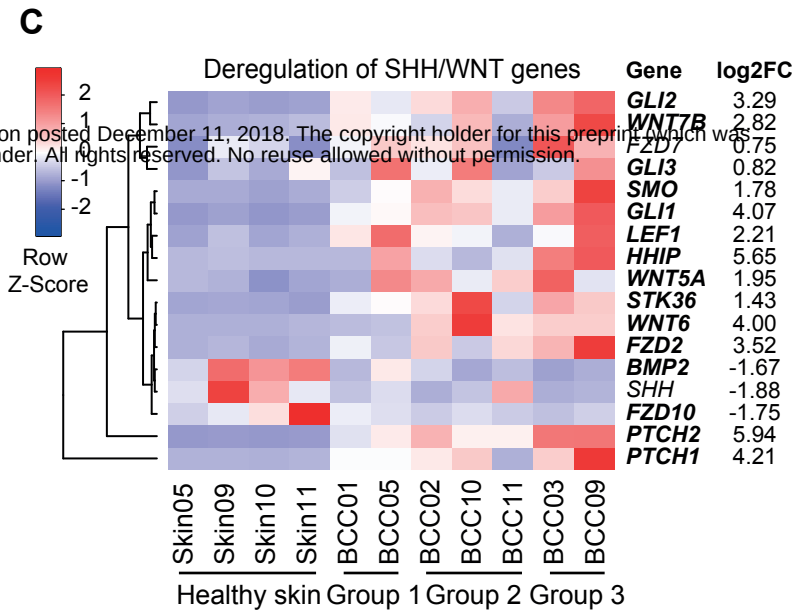

B

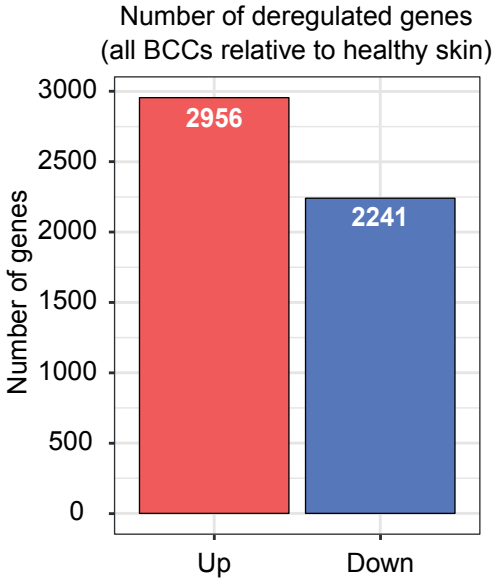

GO-term description	# Genes	FE	FDR
microtubule cytoskeleton organization	158	1.8395	9.8072E-13
skin development	101	2.1761	9.8072E-13
epidermis development	116	2.0349	1.7435E-12
cell projection assembly	153	1.7934	1.6836E-11
cilium organization	106	1.9943	8.5649E-11
cilium assembly	101	1.9791	4.8273E-10
cell cycle phase transition	157	1.6949	8.8240E-10
mitotic cell cycle phase transition	150	1.7156	8.8240E-10
epidermal cell differentiation	74	2.1709	2.3451E-09
microtubule-based movement	86	1.9759	1.7065E-08
homophilic cell adhesion via plasma membrane adhesion molecules	65	2.1498	6.4380E-08
keratinocyte differentiation	56	2.2718	9.0545E-08
cell-cell adhesion via plasma-membrane adhesion molecules	83	1.9240	1.3618E-07
regulation of mitotic cell cycle	148	1.5878	4.0267E-07
mitotic nuclear division	132	1.5793	4.3901E-06
G2/M transition of mitotic cell cycle	67	1.8806	1.5757E-05
cell cycle G2/M phase transition	69	1.8468	2.1387E-05
neural tube development	59	1.9390	2.5589E-05
centrosome organization	45	2.1437	2.8436E-05
autophagy	129	1.5328	3.2914E-05

KEGG pathway	# Genes	FE	FDR
MAPK signaling pathway	81	1.5722	0.0018
Pathways in cancer	114	1.4213	0.0020
Cell cycle	45	1.7962	0.0020
Sphingolipid metabolism	22	2.3169	0.0026
Endocytosis	75	1.4278	0.0261
Phosphatidylinositol signaling system	34	1.6999	0.0329
Inositol phosphate metabolism	26	1.8125	0.0403

Bakker *et al*, Figure 2

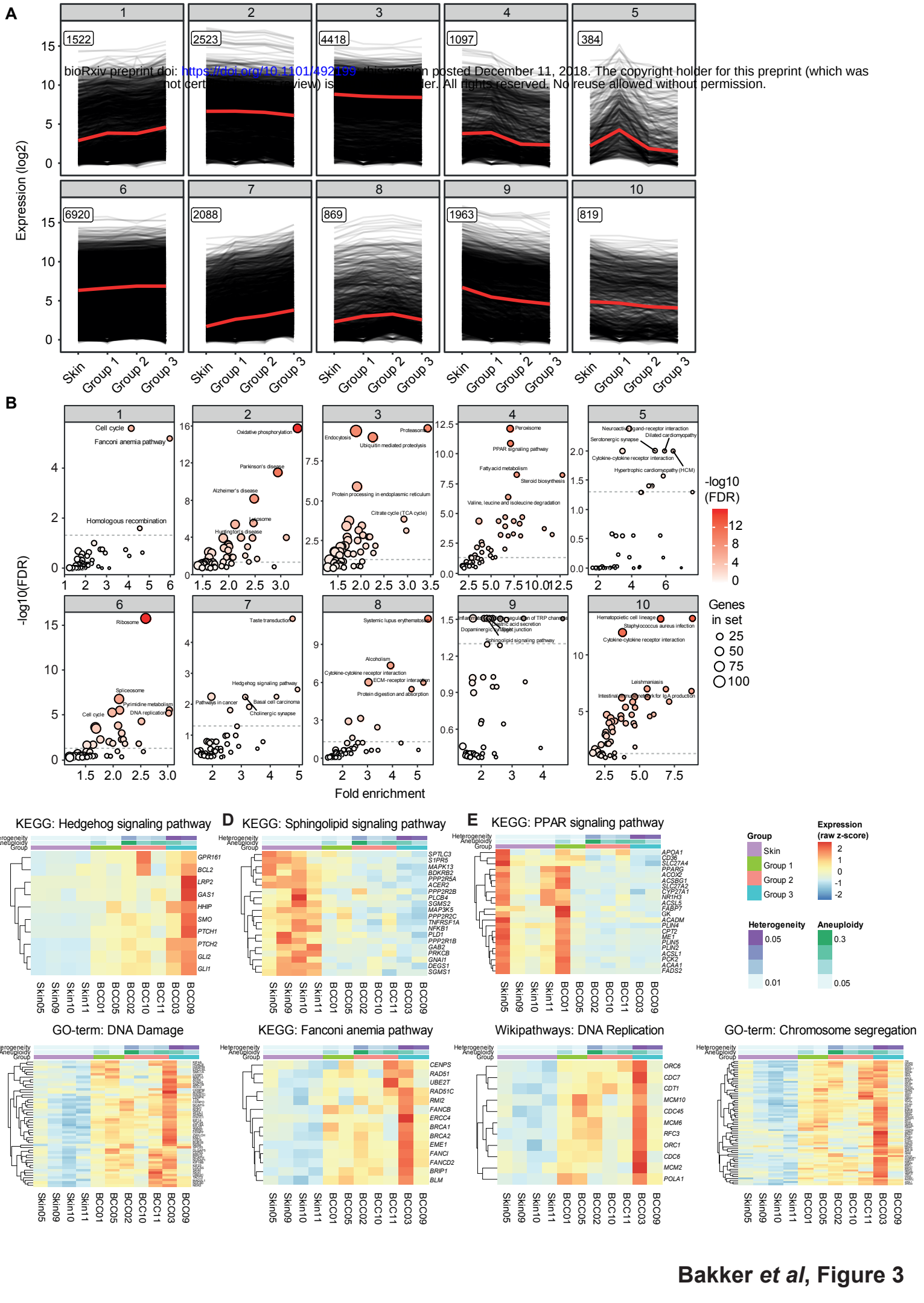

Bakker *et al*, Figure 3

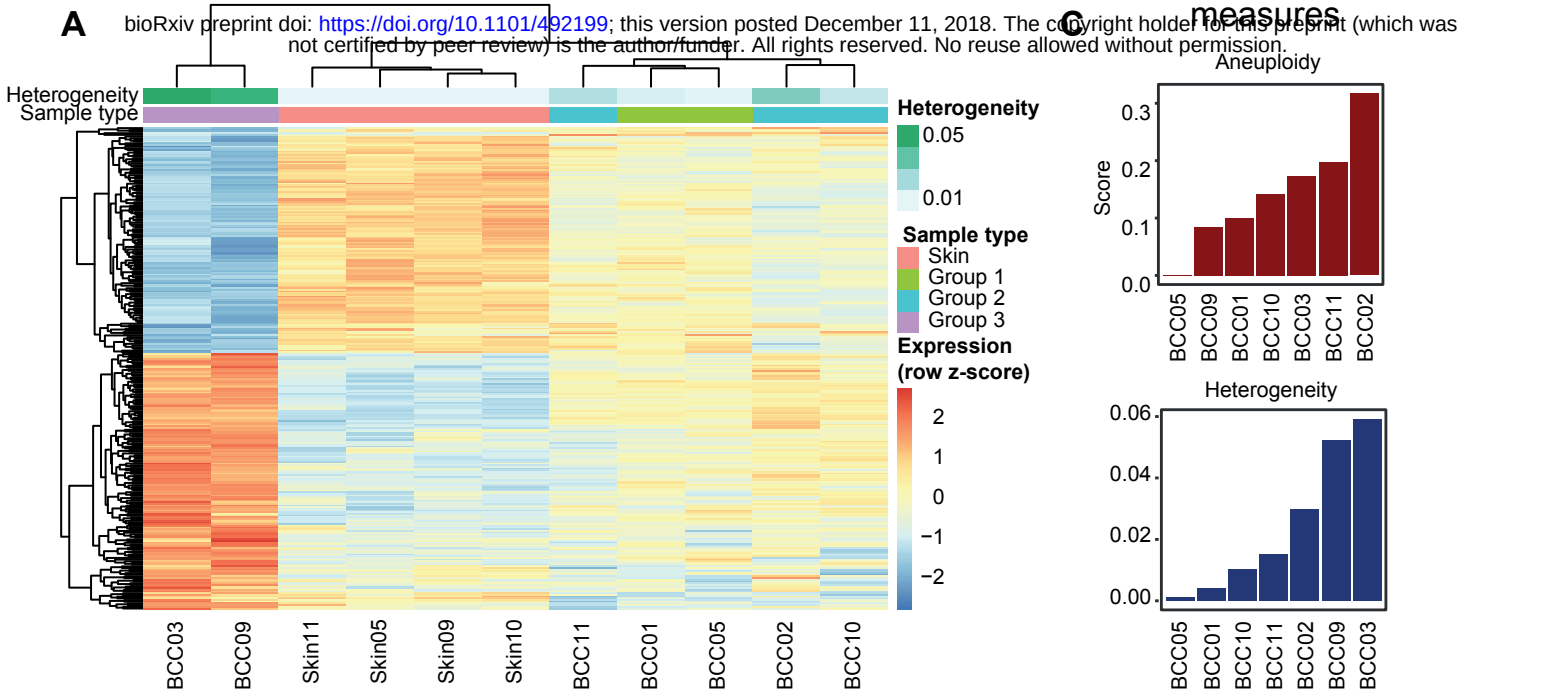

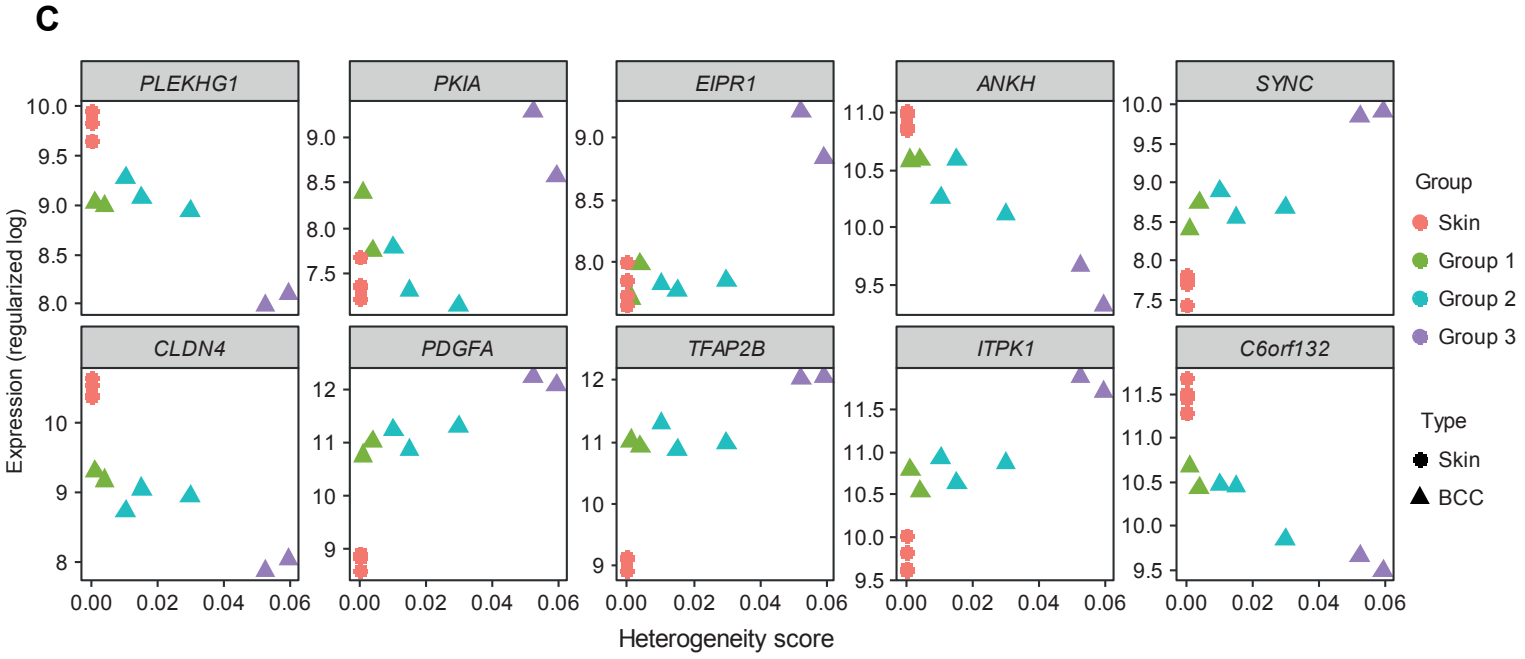

D

GO-term	Number of genes	Fold enrichment	FDR
Cell-cell adhesion via plasma-membrane adhesion molecules	15	5.0171	0.0020
Homophilic cell adhesion via plasma membrane adhesion molecules	11	5.2493	0.0249
Synapse assembly	10	5.2029	0.0456
Calcium-dependent cell-cell adhesion via plasma membrane cell adhesion molecules	5	13.3789	0.0456

Bakker *et al*, Figure 4